

Hydrothermal Synthesis of Er-Doped Luminescent TiO_2 Nanoparticles

Seokwoo Jeon^{†,‡} and Paul V. Braun^{*,‡}

School of Materials Science and Engineering, Seoul National University, Seoul 151-742, Korea, and Department of Materials Science and Engineering, Beckman Institute for Advanced Science and Technology, and Materials Research Laboratory, University of Illinois at Urbana-Champaign, Urbana, Illinois 61801

Received July 18, 2002. Revised Manuscript Received December 27, 2002

Here we report the synthesis and characterization of a stable suspension of fluorescent erbium-doped titania nanoparticles and their assembly into thin films and photonic crystals. The nanoparticles were synthesized through a sol–gel process followed by peptization with tetramethylammonium hydroxide and hydrothermal treatment. As expected, following the hydrothermal treatment, X-ray diffraction shows the particles to be exclusively anatase. The nanoparticles form a stable suspension in water and were cast into 2- and 20- μm -thick films and formed into an inverse opal structure through templating with a colloidal crystal. As synthesized, only a faint fluorescence at 1532 nm was observed from the particles when pumped with 795-nm laser radiation; however, heat treatment at temperatures as low as 100 °C resulted in a significant increase in the fluorescence. The fluorescence was observed to increase further with annealing up to 500 °C, perhaps due to removal of hydroxyl groups and other surface species. Through energy-dispersive X-ray spectroscopy and X-ray diffraction, we present evidence that the Er ions are doped into the TiO_2 nanoparticles and that Er was not present as free Er_2O_3 . This work demonstrates the potential of rare-earth doping of titania nanoparticles for photonic applications.

Introduction

Stable suspensions of rare-earth-doped fluorescent nanoparticles have potential application for the formation of multilayered thin films,¹ optical coatings,² planar waveguides,³ and photonic band gap (PBG)^{4,5} materials. Importantly, light scattering in devices comprised of nanoparticles will be minimized because the nanoparticle diameter is much less than the wavelength of visible or infrared light. Rare-earth doping is interesting because it may result in a strong fluorescence near 1.5 μm , which is the wavelength of interest for many telecommunication applications. Specifically, we have focused on Er-doped titania because there are known routes to stable suspension of TiO_2 nanoparticles^{6–9} and Er-doped TiO_2 has been shown to fluoresce at 1.5 μm .¹⁰

* To whom correspondence should be addressed. E-mail: pbraun@uiuc.edu.

[†] Seoul National University.

[‡] University of Illinois at Urbana-Champaign.

(1) Keddie, J. L.; Braun, P. V.; Giannelis, E. P. *J. Am. Ceram. Soc.* **1993**, 76, 2529.

(2) Linsebigler, A. L.; Lu, G. Q.; Yates, J. T. *Chem. Rev.* **1995**, 95, 735.

(3) Polman, A. *J. Appl. Phys.* **1997**, 82, 1.

(4) Joannopoulos, J. D.; Villeneuve, P. R.; Fan, S. H. *Nature* **1997**, 386, 143.

(5) Joannopoulos, J. D.; Meade, R. D.; Winn, J. N. *Photonic Crystals: Molding the Flow of Light*; Princeton University Press: Princeton, 1995.

(6) Kumar, K. N. P.; Keizer, K.; Burggraaf, A. J.; Okubo, T.; Nagamoto, H.; Morooka, S. *Nature* **1992**, 358, 48.

(7) Cheng, H. M.; Ma, J. M.; Zhao, Z. G.; Qi, L. M. *Chem. Mater.* **1995**, 7, 663.

(8) Burnside, S. D.; Shklover, V.; Barbe, C.; Comte, P.; Arendse, F.; Brooks, K.; Gratzel, M. *Chem. Mater.* **1998**, 10, 2419.

(9) Wang, C.-C.; Ying, J. Y. *Chem. Mater.* **1999**, 11, 3113.

In addition, titania has a high refractive index, 2.4–2.9 depending on the phase,¹¹ which may be important for PBG materials and other photonic applications. In this report, we present for the first time the synthesis and characterization of stable suspensions and films comprised of fluorescent, rare-earth-doped crystalline TiO_2 nanoparticles.

Nanocrystalline titania has been thoroughly studied for applications including photocatalysis,^{2,12} solar energy harvesting,¹³ biological coatings,⁸ and sensors.¹² Commercially, titania powders are generally made by sulfate or chloride methods.¹² However, to form well-dispersed TiO_2 nanoparticles with low polydispersity and high purity, sol–gel routes are promising.^{14,15} One advantage of sol–gel synthesis is that particle size and morphology can be controlled through experimental conditions.^{16–18} Through the introduction of a peptizing agent, aggregation can be eliminated, and the degree of crystallinity is increased.⁶ This peptized product can be subsequently hydrothermally processed at temperatures ranging from

(10) Bahtat, A.; Bouazaoui, M.; Bahtat, M.; Mugnier, J. *Opt. Commun.* **1994**, 111, 55.

(11) Lide, D. R., Ed. *CRC Handbook of Chemistry and Physics*, 81st ed.; CRC Press: Washington, D.C., 2000.

(12) Wang, C.; Deng, Z. X.; Li, Y. *Inorg. Chem.* **2001**, 40, 5210.

(13) Kay, A.; Gratzel, M. *Sol. Energy Mater. Sol. Cells* **1996**, 44, 99.

(14) Brinker, C. J.; Scherer, G. W. *Sol–Gel Science: the physics and chemistry of sol–gel processing*; Academic Press: San Diego, 1990.

(15) Dislich, H.; Hinz, P. *J. Non-Cryst. Solids* **1982**, 48, 11.

(16) Wang, Y.; Cheng, H.; Hao, Y.; Ma, J.; Li, W.; Cai, S. *Thin Solid Films* **1999**, 349, 120.

(17) Scolan, E.; Sanchez, C. *Chem. Mater.* **1998**, 10, 3217.

(18) Chemseddine, A.; Moritz, T. *Eur. J. Inorg. Chem.* **1999**, 235.

80 to 300 °C, resulting in a stable suspension of crystalline particles.^{7–9,18–22} This suspension can be self-organized into films⁸ and superlattice structures.¹⁸

Titania exists in three polymorphs: anatase, rutile, and brookite. Although the rutile phase is most thermodynamically stable, anatase is generally found for sol–gel-derived titania for kinetic reasons. However, it must be noted that rutile is denser and has a greater refractive index, which may be important for PBG and other applications. The anatase to rutile phase transition usually requires a heat treatment of 600–1100 °C.^{22,23} Recently, however, for the PBG applications, there have been several attempts to decrease the transition temperature. It was shown that a low pH promotes the formation of the rutile phase, especially when peptization is conducted with HNO_3 at room temperature.^{7,21} In contrast, organic bases such as tetraalkylammonium hydroxides generally result in anatase.

Titania films can be formed both directly from sol–gel precursors and from nanoparticle solutions.^{1,24} For photonic and electrochemical applications, it is often important that these coatings be relatively thick (>1 μm) and thermally and mechanically stable. When formed through a sol–gel route, however, films thicker than 1 μm are generally unstable.¹ Films derived from nanoparticle sols can be much thicker because they undergo less shrinkage during drying and thus the stress on the dry film is considerably reduced.

Rare-earth-doped fibers and films are becoming increasingly important for application as waveguides and amplifiers.³ Specifically, erbium in its trivalent state has a strong fluorescence around 1.53 μm , which falls within one of the transmission windows in silica, and thus is commonly used in optical telecommunications.^{3,10,25} The formation of Er-doped TiO_2 planar waveguides through a sol–gel process has been demonstrated.^{10,26,27} TiO_2 was selected as the host because it has lower phonon energies than silica, which may help to increase the probability of radiative transitions.^{10,25} These waveguides had a strong emission peak at 1.53 μm when excited by 800-nm radiation.¹⁰

To the best of our knowledge, there has been no research on Er or any other rare-earth-doped TiO_2 nanoparticles. For thin film (<1 μm) applications, sol–gel-derived Er-doped TiO_2 is satisfactory. Ion implantation, beam epitaxies, and electrochemical methods can also be used to rare-earth dope thin films.^{3,28} However, these methods cannot be used for thick film or bulk

applications. For such applications, well-dispersed rare-earth-doped nanocrystals are very attractive. Here we demonstrate hydrothermal processing as a route to create such nanocrystals. Hydrothermal processing has long been utilized to make advanced ceramic powders with controlled homogeneity and properties at relatively low cost,^{29–31} and more recently, it has been investigated for the formation of luminescent materials for displays.^{32,33}

Because the conventional luminescent particle preparation methods of sol–gel, coprecipitation, and solid-state reactions require calcination and milling, which result in agglomerate formation and degradation of the surface, hydrothermal processing has been studied as a route to dope activator ions into an inorganic host matrix.^{32,33} Hydrothermal processing both maintains the particles in solution throughout the process and allows a high-temperature step to anneal out defects, which can result in better luminescence properties. A good example is the manganese doping of willemite through hydrothermal synthesis to form a green phosphor.³² In our scheme we add Er to the peptized sol–gel precursor and then hydrothermally process the mixture at elevated temperature and pressure to activate the Er.

A novel application of Er-doped nanocrystalline titania may be in PBG materials. Several groups have demonstrated the formation of macroporous photonic crystals comprised of titania through the imbibing of TiO_2 nanoparticles into a colloidal crystal, followed by removal of the colloidal template.^{34–36} TiO_2 is interesting because of its relatively high refractive index (2.4–2.9)¹¹ and high transparency in the visible and IR. It should be noted that infiltration of colloidal crystals with sol–gel is not as effective as nanoparticle infilling for forming an inverse opal because it results in a low-density structure with a lower effective refractive index.^{34,35,37–39} Rare-earth-doped TiO_2 nanoparticles specifically may be interesting for PBG applications because of the potential for the added optical functionality which results from Er doping.

Experimental Section

(19) Yang, J.; Mei, S.; Ferreira, J. M. F. *J. Am. Ceram. Soc.* **2001**, *84*, 1696.
 (20) Yang, J.; Mei, S.; Ferreira, J. M. F. *Mater. Sci. Eng. C* **2001**, *15*, 183.
 (21) Yang, J.; Mei, S.; Ferreira, J. M. F. *J. Am. Ceram. Soc.* **2000**, *83*, 1361.
 (22) Yanagisawa, K.; Ovenstone, J. *J. Phys. Chem. B* **1999**, *103*, 7781.
 (23) Ovenstone, J.; Yanagisawa, K. *Chem. Mater.* **1999**, *11*, 2770.
 (24) Ohya, Y.; Mishina, J.; Matsuda, T.; Ban, T.; Takahashi, Y. *J. Am. Ceram. Soc.* **1999**, *82*, 2601.
 (25) Mignotte, C. *J. Non-Cryst. Solids* **2001**, *291*, 56.
 (26) Bahtat, A.; deLucas, M. C. M.; Jacquier, B.; Varrel, B.; Bouazaoui, M.; Mugnier, J. *Opt. Mater.* **1997**, *7*, 173.
 (27) Bahtat, A.; Bouderbala, M.; Bahtat, M.; Bouazaoui, M.; Mugnier, J.; Druetta, M. *Thin Solid Films* **1998**, *323*, 59.
 (28) Gaponenko, N. V.; Sergeev, O. V.; Stepanova, E. A.; Parkun, V. M.; Mudryi, A. V.; Gnaser, H.; Misiewicz, J.; Heiderhoff, R.; Balk, L. J.; Thompson, G. E. *J. Electrochem. Soc.* **2001**, *148*, H13.

(29) Morey, G. W. *J. Am. Ceram. Soc.* **1953**, *36*, 279.
 (30) Dawson, W. *J. Am. Ceram. Soc. Bull.* **1988**, *67*, 1673.
 (31) Yoshimura, M.; Suchanek, W. L.; Byrappa, K. *MRS Bull.* **2000**, *25*, 17.
 (32) Yoon, C.; Kang, S. *J. Mater. Res.* **2001**, *16*, 1210.
 (33) Li, Q. H.; Komarneni, S.; Roy, R. *J. Mater. Sci.* **1995**, *30*, 2358.
 (34) Subramanian, G.; Manoharan, V. N.; Thorne, J. D.; Pine, D. J. *Adv. Mater.* **1999**, *11*, 1261.
 (35) Subramanian, G.; Constant, K.; Biswas, R.; Sigalas, M. M.; Ho, K. M. *Appl. Phys. Lett.* **1999**, *74*, 3933.
 (36) Vlasov, Y. A.; Yao, N.; Norris, D. J. *Adv. Mater.* **1999**, *11*, 165.
 (37) Wijnhoven, J.; Vos, W. L. *Science* **1998**, *281*, 802.
 (38) Holland, B. T.; Blanford, C. F.; Stein, A. *Science* **1998**, *281*, 538.
 (39) Braun, P.; Wiltzius, P. *Adv. Mater.* **2001**, *13*, 482.

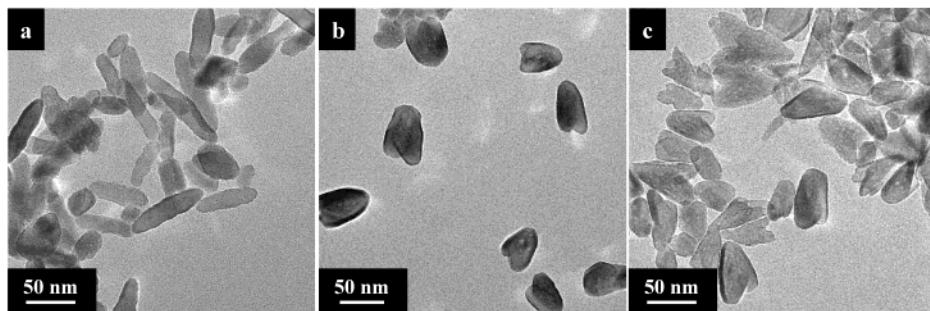


Figure 1. TEM micrographs of erbium-doped titania nanoparticles: 1 mol % (a), 2 mol % (b), and 3 mol % (c) Er^{3+} . For all three samples the hydrothermal H_2O ratio is 1:41.7.

peptization was performed at 85 °C for 1 h in a closed container with vigorous stirring. Then 2 mL of an aqueous solution of erbium nitrate pentahydrate ($\text{Er}(\text{NO}_3)_3 \cdot 5\text{H}_2\text{O}$, Acros) was added dropwise to this mixture and stirring was continued for 30 min at the same temperature. The mole percent of Er with respect to Ti was set to 1, 2, or 3%. Including all added water, the final Ti-to-water ratio (hydrothermal H_2O ratio) was 1:41.7, 1:83.3, 1:167, or 1:333. Within 1 h of the start of peptization, the slurry became less opaque. The peptized, Er-containing mixture was placed in a Teflon liner, docked into an acid digestion bomb (4746, Parr), and held at 210 °C for 3 h. As previously reported, the solution became opaque due to particle growth.⁸

The final product was purified through centrifugation (J2-21, Beckman). There were two types of samples depending on the hydrothermal water ratio, a wet sediment, and a nanoparticle suspension. The 1:41.7 hydrothermal H_2O ratio resulted in a material that sedimented under gravity and was used to prepare powder samples. The stable suspension resulting from the 1:83.3 hydrothermal H_2O ratio was selected to form film samples. Both were purified with DI water to remove excess TMNH and reaction byproducts. The 1:41.7 samples would sediment under gravity, but were centrifuged to accelerate the process, and the 1:83.3 samples required centrifugation at 4000×*g* for 1 h to sediment. Following each centrifugation, the supernatant was removed, and the samples were sonicated in fresh DI water to disperse the nanoparticles. The process of centrifugation and sonication was repeated three times. The purified sediments from the 1:41.7 ratio sample were dried to powder in an oven at 70 °C. The purified nanoparticle suspension from the 1:83.3 ratio sample was concentrated to 5 wt % in DI water by resuspending with minimal water after the last washing, and films were formed by casting the suspension on glass substrates.

Photonic Crystal Preparation. A colloidal crystal was self-assembled from 466-nm-diameter carboxyl/sulfate-terminated polystyrene particles (IDC), and the Er-doped TiO_2 nanoparticle suspension from the 1:83.3 ratio was cast on top of it. Following drying at room temperature, the sample was calcined at 300 °C for 1 h in air to remove the polystyrene template.

Characterization. A tunable Ti:sapphire laser was used as the excitation source for photoluminescence (PL) studies. The excitation wavelength was 795 nm, which was the absorption maximum for the sample. The laser was mechanically chopped at 40 Hz. A germanium detector (EO-817L, North Coast), cooled at 77 K, and a 1-m single grating monochromator were used with a lock-in amplifier to amplify the signal. All experiments were performed at room temperature.

The phase, size, and crystallinity of the Er-doped titania were analyzed by X-ray diffraction (XRD) (Rigaku RU200), using Cu K α radiation, scanning electron microscopy (SEM) (Hitachi S-4700), and transmission electron microscopy (TEM) (Philips CM12). TEM samples were prepared by applying a diluted drop of particles on a holey carbon-coated copper TEM grid (SPI). Energy-dispersive X-ray (EDX) data demonstrating the Er doping of the nanoparticles was acquired using both the Philips CM12 for a cluster of particles and JEOL 2010F

Table 1. EDX Data Collected from the 3% Erbium-Doped Titania Nanoparticles (1:83.3 Hydrothermal H_2O Ratio)^a

sample	at. % Ti	at. % Er	sample	at. % Ti	at. % Er
S1	97.35	2.65	S5	99.29	0.71
S2	99.7	0.3	S6	97.68	2.32
S3	99.09	0.91	C1	95.84	4.16
S4	97.42	2.58	C2	97.42	2.58

^a The oxygen signal was not included in the analysis.

in scanning transmission electron microscopy (STEM) mode for single particles and a cluster. Thermogravimetric analysis (TGA) was performed using a Mettler Toledo TGA/SDTA851 from room temperature to 800 °C.

Results and Discussion

Nanoparticle and Film Structure. There have been many attempts to control the hydrolysis and condensation of titanium alkoxides because of their high reactivity.^{9,17–19,40} In this study, however, our goal is the synthesis of relatively large well-dispersed Er-doped TiO_2 nanoparticles, and thus control of hydrolysis conditions was not critical. In this work, a simple hydrolysis with water was utilized and an autoclaving temperature of 210 °C was chosen because this temperature has been reported to be sufficient for the formation of highly crystalline anatase nanoparticles.⁸

As the doping ratio of erbium was increased from 1 to 3 mol %, the morphology of particles changed. At 1 mol % Er, the nanoparticles are elongated as shown in Figure 1a, which is similar in morphology to undoped TiO_2 .⁸ Parts (b) and (c) of Figure 1, 2 and 3 mol % Er, respectively, show nanoparticles that are more spherical or triangular in shape. We suspect the morphology change is related to the erbium doping. It has previously been suggested that Er^{3+} strongly affects the crystallization of sol–gel-derived titania by stabilizing amorphous material.²⁷ Additionally, perhaps Er^{3+} hinders the growth of specific facets of anatase TiO_2 .

The coordination of Er ions in Er-doped titania has not been fully resolved; however, recent research on sol–gel titania doped with 15% Er revealed no erbium oxide aggregates in the TiO_2 matrix.²⁵ Because the product of our synthesis is well-dispersed nanoparticles, the presence of the Er could be investigated through EDX analysis. Initial EDX data on a cluster of particles was collected using a conventional TEM, indicating the Er doping was 4.16 at. % relative to Ti for the 3% erbium-doped titania nanoparticles (Table 1, Figure 2, sample C1). However, because this is a cluster of particles, there is the possibility that some Er was present as isolated erbium oxide particles. Through the use of STEM with

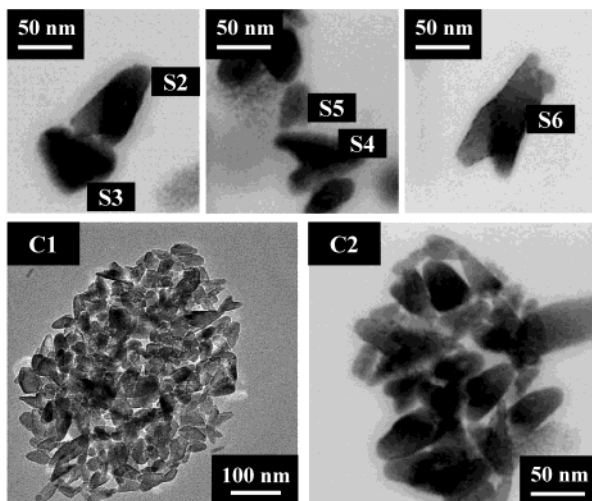


Figure 2. TEM micrographs of particles and clusters from which the data in Table 1 were obtained.

a beam diameter below 0.6 nm, a precise measurement of the Er content of single nanoparticles was determined. As presented in Table 1, the atomic percent of erbium varies from 0.3 to 2.65% for individual nanoparticles (samples S1–S6 shown in Figure 2), and the doping for a cluster of nanoparticles was 2.58% (Figure 2, sample C2). As previously mentioned, the nanoparticle shape changed from rodlike to triangular with Er doping, which might indicate that the Er concentration is dependent on the crystallographic orientation of titania particles. Thus, perhaps the concentration of Er varies spatially, even within a single nanoparticle; since the beam is much smaller than the particle, this might explain the observed variation. From these observations and diffraction studies that will be presented shortly, we conclude that the erbium exists as a dopant of the TiO_2 nanoparticles and is not present as isolated free material.

Various mole ratios of $H_2O:Ti$ were tested to determine which yielded the best dispersion after hydrothermal processing; 1:41.7, 1:83.3, 1:167, and 1:333 were tested. The ratio of 1:83.3 consistently yielded the best dispersion. It has been reported that as long as the H_2O :alkoxide ratio is greater than 50, hydrothermal treatment promotes crystallization of nanoparticles.⁹ Although most groups use the same hydrothermal H_2O ratio as the initial hydrolysis ratio throughout the experiment, the hydrothermal H_2O ratio of our system was varied to identify the optimal condition for dispersion of the nanoparticles. The initial hydrolysis ratio of all the samples was above 150, so nearly complete hydrolysis and condensation are expected. After the hydrothermal treatment, all the solutions except the 1:83.3 ratio at least partially sedimented to the bottom of the bottle; however, the solution with the 1:83.3 ratio was quite stable and only trace sediment was observed, suggesting this ratio results in an optimal pH and concentration for obtaining well-dispersed nanoparticles in solution. In all cases, a 0.25 mole ratio of TMNH to titanium was used; however, because of the different volumes of water used, the hydrothermal processing solution had different chemical concentrations and pH, which may have been the cause of sediment formation in some of the systems. It has been reported that for

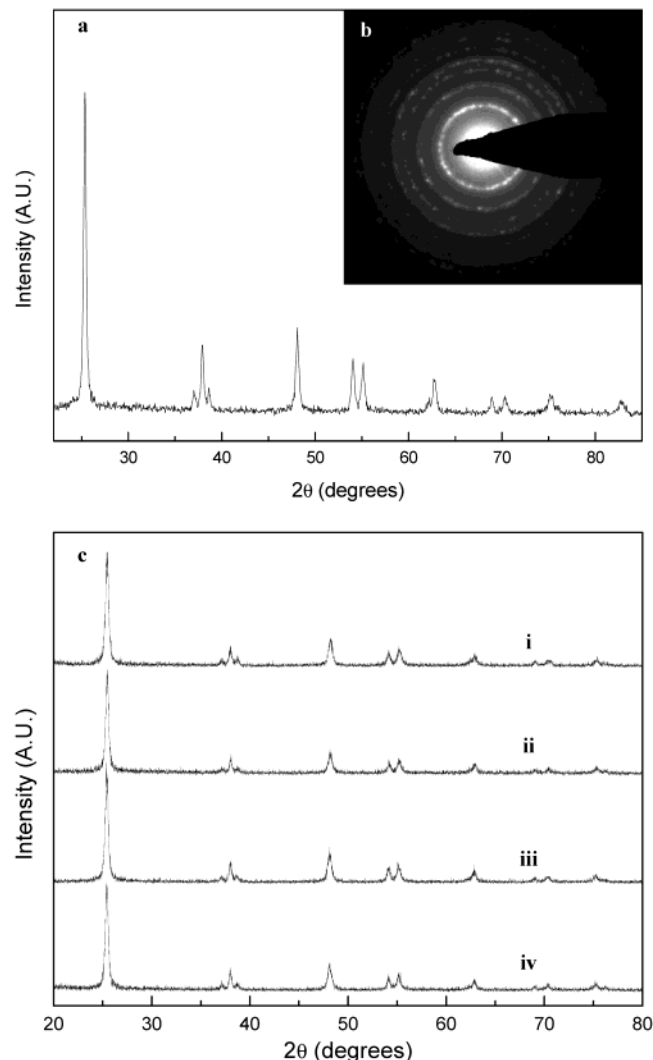


Figure 3. (a) XRD data obtained from 3% erbium-doped titania sediment (1:41.7 hydrothermal H_2O ratio), (b) SAD from 3% erbium-doped nanoparticles (1:83.3 hydrothermal H_2O ratio), (c) XRD data from films of 3% erbium-doped nanoparticles (1:83.3 hydrothermal H_2O ratio) heat-treated at (i) 500 °C, (ii) 300 °C, (iii) 100 °C, and (iv) room temperature.

higher concentrations of peptizing agent more significant agglomerates were formed,²⁰ which may explain the formation of aggregates in the 1:41.7 ratio system. However, a detailed investigation of the mechanism for particle stabilization was not part of this study.

As expected, our system, peptized by the organic base TMNH, crystallized as anatase. XRD data and SAD are characteristic of anatase (Figure 3). All the peaks of the XRD pattern index to anatase phase and no peaks of the rutile or brookite phase were observed. Additionally, no peaks from erbium oxide were observed. According to the Scherrer equation, the (101) anatase peak of Figure 3a indicates an average particle size of ~30 nm, which is consistent with the grain size observed by TEM and SEM. Figure 3c is XRD data from 20- μ m-thick film samples that were used for fluorescence studies. These measurements indicate no phase transformation up to at least 500 °C, and from the Scherrer equation for the (101) anatase peak, no significant change in particle sizes was found due to annealing.

Films were formed by casting a 5 wt % particle solution in water on a cover glass followed by drying at

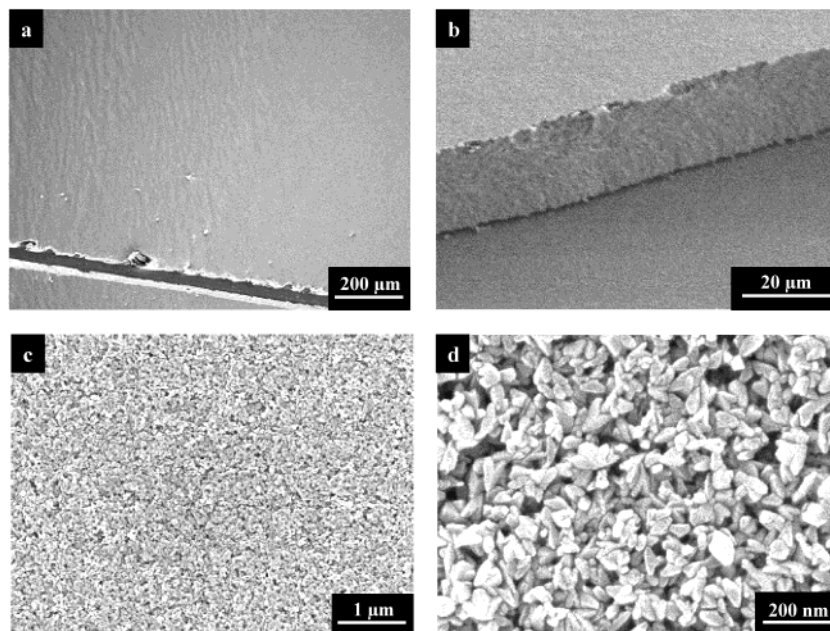


Figure 4. SEM micrographs of a 3% Er-doped TiO_2 film dried on a cover glass. Top view of the film along an intentional scratch (a), 45° tilted view showing the film thickness (b), and high-resolution top views of the film (c, d).

room temperature. After drying, the films were translucent. The scratch at the bottom of the SEM in Figure 4a was intentionally made to determine the thickness of the film. It should be noted that there was no crack formation around the scratch, indicating the film is mechanically stable. In Figure 4b, the thickness of the film is shown to be about 20 μm and that the structure through the film is uniform. The film also appeared uniform and flat in higher magnification images (Figure 4c,d) and no skin on the surface of the film was observed, which would have been indicative of impurities in the nanoparticle suspension. Thus, it appears that, prior to heat treatment, a film prepared from the Er-doped nanoparticles is very stable, even in thick film form. After heat treatment, the films were cracked into domains on average 100- μm across (Figure 5a-c). Because this cracking occurs for even the lowest temperature heat treatment of 100 °C, it is likely the result of the slight contraction due to the removal of physisorbed water on the surface of nanoparticles. After heat treating to 300 and 500 °C, the cracks appear a bit wider, which is probably due to the removal of the TMNH groups from the surface of the particles. As these films were quite thick (~20 μm), cracking most likely cannot be avoided. Thinner films (~2 μm) formed by casting a 0.5 wt % nanoparticle solution did not crack, even after heat treatment at 300 or 500 °C (Figure 5d,e). It appears the stress developed in these films is not significant enough to lead to cracking.

Luminescence. The fluorescence of erbium within the titania matrix originates from an excited ${}^4\text{I}_{9/2}$ state. The emission at 1.53 μm is the radiative transition of ${}^4\text{I}_{13/2}$ to ${}^4\text{I}_{15/2}$.^{10,25} The electronic energy level of trivalent erbium ion in silica is reported to be about 800 nm for ${}^4\text{I}_{9/2}$ and about 1530 nm for ${}^4\text{I}_{13/2}$ relative to ${}^4\text{I}_{15/2}$.^{41,42} This $4\text{f} \leftrightarrow 4\text{f}$ transition is actually forbidden by the

parity selection rule, but is allowed to some extent by the crystal field of the host matrix.^{43,44} In general, optical transitions of rare-earth ions are relatively unperturbed by the crystal field of the host lattice because the 5s5p electrons shield the 4f electrons of the rare-earth atom.^{43,44} So 795-nm radiation from a Ti:sapphire laser was chosen for excitation because the strongest emission at 1532 nm was detected from this wavelength. Though the host matrix does not greatly influence the transitions of erbium, the emission wavelength of Er-doped glasses has been reported to vary from 1530.6 to 1535.8 nm depending on the host.⁴²

Fluorescence of Er-doped TiO_2 powders was collected from particles obtained from the sediment of the 1:41.7 hydrothermal H_2O ratio. The fluorescence from a bulk sample of the 3 mol % of Er-doped powders shows a sharp fluorescence peak at 1532 nm (Figure 6); 20- μm -thick films made of 3 mol % of Er-doped nanoparticles from the stable suspension resulting from the 1:83.3 hydrothermal H_2O ratio were also characterized. The titania films made from these nanoparticles yielded relatively weak fluorescence before heat treatment (Figure 7a). SEM revealed no intrinsic differences between the nanoparticles composing the powders and the film, and thus the stronger fluorescence of the powder is both because the powder had an essentially infinite thickness compared to the film and because of the waveguide effect of the film. A flat film with a refractive index of 2.4 at the emission wavelength will totally internally reflect 80% of the emission assuming isotropic emission, preventing it from being detected. Some of the trapped photons may be subsequently scattered out of the film, but at 1.5 μm , this scattering may be weak. Regardless, the film thickness should have been sufficient to generate a strong luminescence. Most probably, the hydroxyl groups on the surface of

(40) Vorkapic, D.; Matsoukas, T. *J. Am. Ceram. Soc.* **1998**, *81*, 2815.
 (41) Sanghera, J. S.; Sagarwal, I. D. *Infrared Fiber Optics*; CRC Press: Boca Raton, FL, 1998.
 (42) Miniscalco, W. J. *J. Lightwave Technol.* **1991**, *9*, 234.

(43) Blasse, G.; Grabmaier, B. C. *Luminescent Materials*; Springer-Verlag: Berlin, 1994.

(44) Vij, D. R. *Luminescence of Solids*; Plenum Press: New York, 1998.

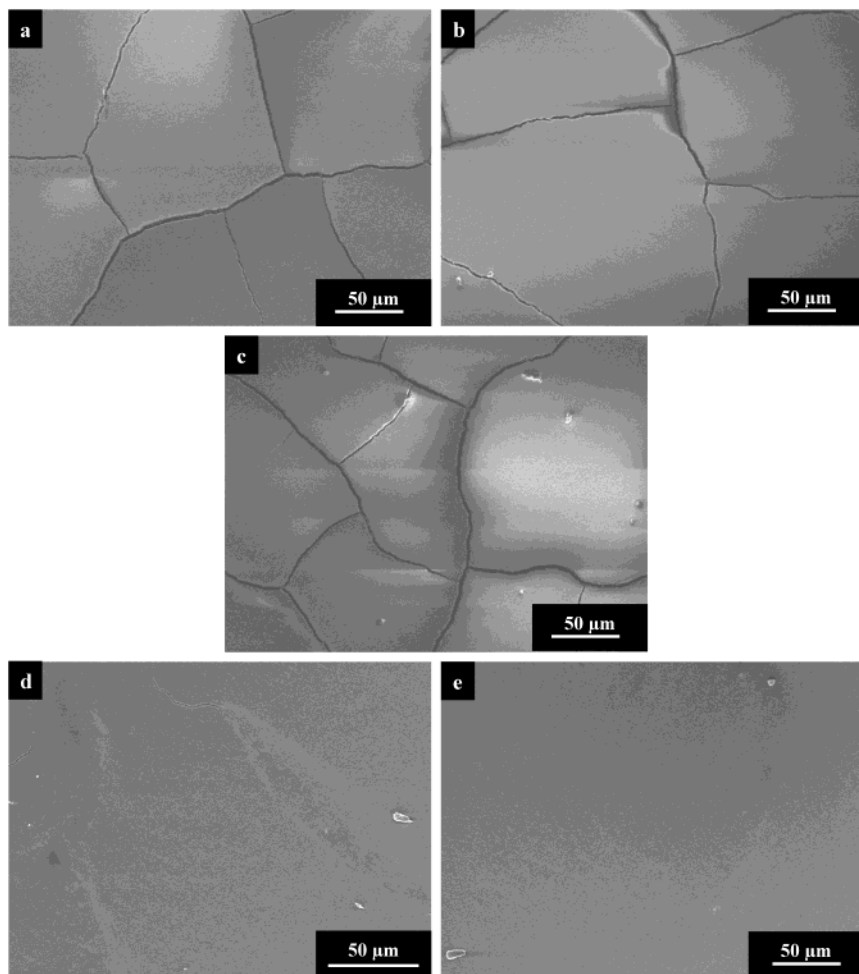


Figure 5. SEM micrographs of 20- μ m-thick films heat-treated at 100 °C (a), 300 °C (b), and 500 °C (c). SEM micrographs of 2- μ m-thick films heat-treated at 300 °C (d) and 500 °C (e).

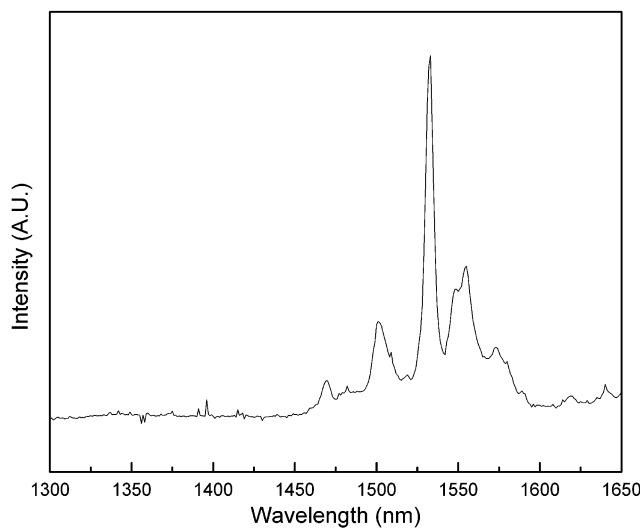


Figure 6. Fluorescence spectra of 3% Er-doped TiO_2 powder obtained from the dried sediment of the 1:41.7 hydrothermal H_2O ratio.

titania lead to nonradiative decay of excited erbium ions.²⁶ To remove adsorbed species, the films were heat-treated at 100, 300, and 500 °C for 1 h in air. The films were uniform and translucent after drying and heat treatment. The fluorescence data from the heat-treated samples are presented in Figure 7b–d. A peak at 1532

nm was observed from all of the samples. Because the intensity of fluorescence strongly depends on the condition of measurement and focusing, an absolute intensity of fluorescence was not determined. However, the intensity of emission is clearly stronger after the higher temperature heat treatments. For example, the emission from the sample heat-treated at 500 °C is about twice that of the sample treated at 300 °C, and on the order of 10 times that of the room-temperature sample. In fact, it was similar to that of the powder samples shown in Figure 6. Further work to quantify the intensity of the emission will be reported in a subsequent publication.

We suspect the increase in fluorescence after heat-treating is due to desorption of water and hydroxyl groups (Ti–OH). There are two types of water on an anatase surface. Type I is hydrogen bound to surface hydroxyl, and type II is hydrogen bound to surface oxygen.¹ Both desorb under 250 °C, but partial rehydration is possible when the heat treatment is less than 500 °C.¹ The increase in luminescence intensity after heat treatment suggests that some desorbable species favors nonradiative relaxations of Er. Hydroxyl groups are known to increase the probability of nonradiative relaxations of erbium ions; thus, it has been suggested the removal of hydroxyl groups by heat treatment will increase the lifetime of the excited state, thus increasing the fluorescence.²⁶ TGA was performed to determine the

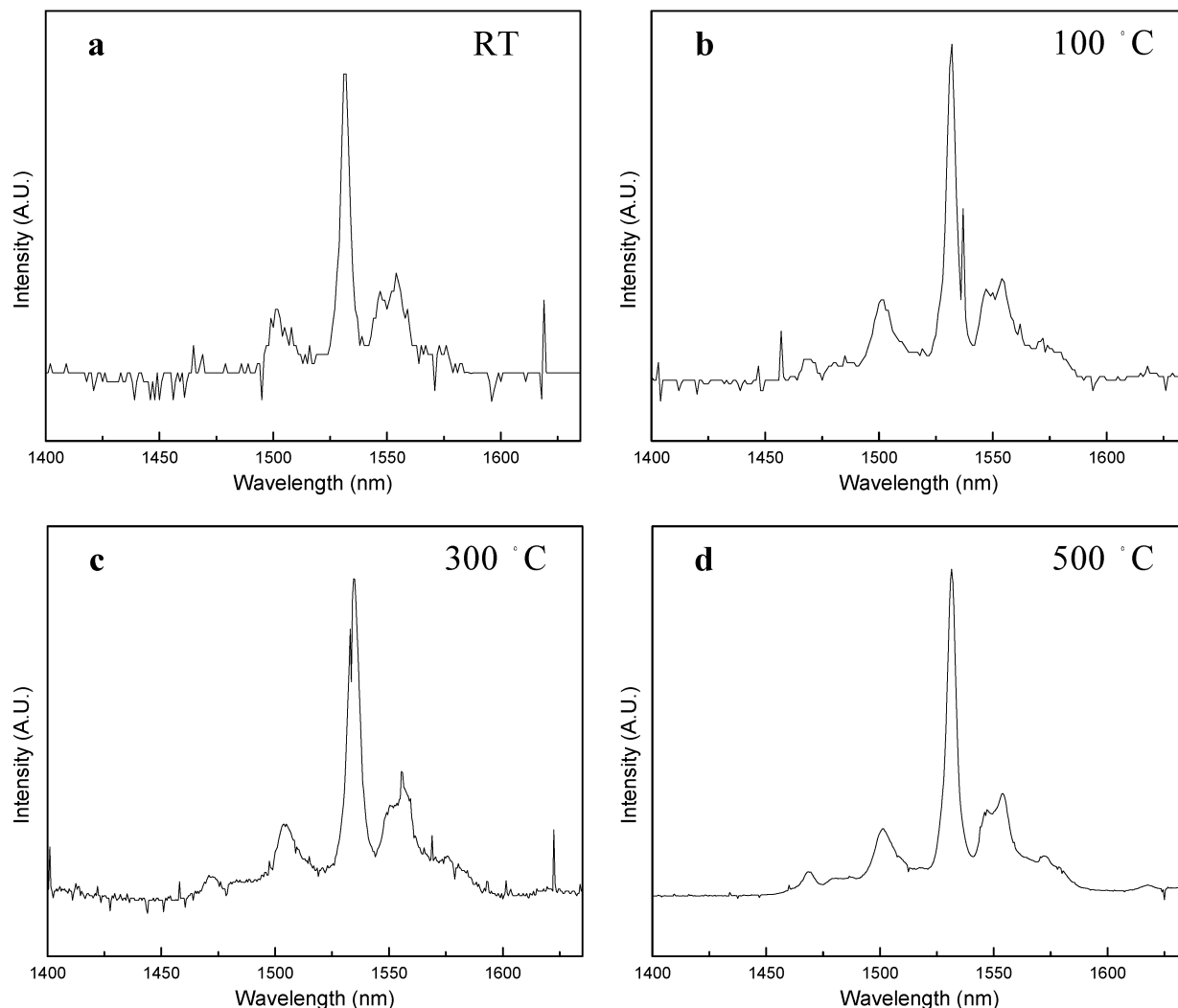


Figure 7. Fluorescence spectra of $\sim 20\text{-}\mu\text{m}$ -thick erbium-doped titania films. All four samples were from the 3% erbium-doped nanoparticles synthesized with the 1:83.3 hydrothermal H_2O ratio. Dried at room temperature (a), heat-treated for 1 h at 100 $^{\circ}\text{C}$ (b), 300 $^{\circ}\text{C}$ (c), and 500 $^{\circ}\text{C}$ (d).

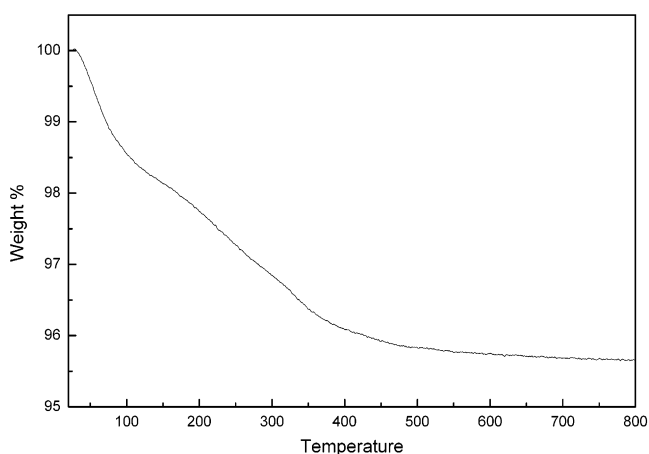


Figure 8. TGA data obtained from 3% Er-doped TiO_2 synthesized with the 1:83.3 hydrothermal H_2O ratio.

desorption temperature of various species. The results indicate there was about 4% weight loss from room temperature to 500 $^{\circ}\text{C}$, and little weight loss after that (Figure 8). By 100 $^{\circ}\text{C}$ a luminescence can be regularly observed; however, it does not become strong until the films are heated to greater than 300 $^{\circ}\text{C}$. The weight loss from room temperature to 100 $^{\circ}\text{C}$ is almost certainly

from removal of water, while we suspect the weight loss above 100 $^{\circ}\text{C}$ is due to removal of water, TMNH, and perhaps hydroxyl groups. Full decomposition of hydroxyl groups requires a heat treatment around 1000 $^{\circ}\text{C}$,²⁰ however, we see little weight loss between 500 and 800 $^{\circ}\text{C}$, so we believe only trace structural water is present at 500 $^{\circ}\text{C}$ since most would likely be removed by 800 $^{\circ}\text{C}$.

From the sharp emission peak at 1532 nm we can conclude Er^{3+} ions are stable in the nanoparticles and that the inhomogeneous broadening due to an amorphous host or surface states does not occur.⁴³ It is possible that the Er could exist as a free oxide form; however, the reported fluorescence of erbium oxide nanoclusters synthesized through a micro emulsion technique was centered at 1540 nm and had a fwhm of 22 nm.⁴⁵ In contrast, our nanoparticles exhibited a sharp peak at 1532 nm with a fwhm of 5 nm, adding further weight to our belief that the Er ions are present in the TiO_2 matrix, and not as a free species.

Colloidal Templating. To demonstrate the possibility of incorporating the Er-doped nanoparticles in pho-

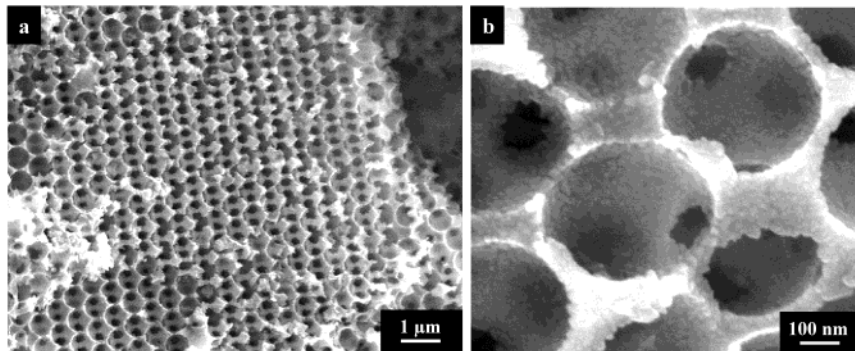


Figure 9. SEM micrographs of macroporous titania structure templated using a colloidal crystal formed from 466-nm polystyrene colloidal particles: (a) low magnification; (b) high magnification.

tonic crystal applications, the nanoparticles were infiltrated into a polystyrene colloidal crystal. Following removal of the colloidal crystal, it can be seen that the nanoparticles filled the interstitial sites of the colloidal crystal (Figure 9). High-magnification SEM (Figure 9b) revealed that the nanoparticles filled the interstitial voids of the polystyrene colloidal crystals except for a small region around the contact points of the spheres. In addition it can be seen that the TiO_2 nanoparticles preserved the structure of the colloidal template, even after removal of the template through calcination.

Conclusions

We have developed a new route to synthesize fluorescent Er-doped TiO_2 nanoparticles through a simple hydrothermal method starting from sol–gel precursors. Strong 1532-nm infrared fluorescence was observed from a powder of the 3 mol % Er-doped particles when excited by 795-nm radiation. A stable suspension of nanoparticles in solution was achieved by using 25 mol % of the peptizing agent TMNH with respect to titanium and selecting a 1:83.3 Ti:H₂O ratio for hydrothermal processing. The hydrothermal synthesis yielded a stable dispersion in water of highly crystalline Er-doped particles with an average particle size of about 50 nm from the TEM and SEM analysis. The Er doping leads to a change in the morphology of nanoparticles from rodlike to triangular as the Er-doping ratio to Ti increased from 1 to 3 mol %, which may be the result of

the Er ions inhibiting the growth of specific facets of the TiO_2 particles. Strong fluorescence from thin films of the nanoparticles could be achieved by annealing at 500 °C, while as deposited films had little fluorescence, indicating the possibility of luminescence quenching by removable surface hydroxyl groups. From the fluorescence, XRD, and EDX data, it could be concluded that Er³⁺ is doped into the anatase phase nanoparticles and is not present as free Er oxide. The particles form uniform translucent films and are small enough to be imbibed into colloidal crystals for PBG applications. With these desirable properties, rare-earth-doped nanoparticles may find application in optical films, infrared lasers, and PBG materials as a luminescent material.

Acknowledgment. This work was supported by the Brain Korea 21 program of Materials Education and Research Division at Seoul National University, the U.S. DOE, Division of Materials Sciences under Award No. DEFG02-91ER45439, through the Frederick Seitz Materials Research Laboratory at the University of Illinois at Urbana-Champaign, and the Nanoscale Science and Engineering Initiative of the NSF under Award No. DMR-0117792. We thank A. Mitofsky for assistance with photoluminescence spectroscopy, Dr. R. Tweten for assistance with EDX analysis on the JEOL 2010F, and Prof. S. Kang at SNU for advice.

CM0207402